How and when can environmental influences change cerebral cortex? An experimental training study of twins with birth weight differences

Kristine B Walhovd*[1,2], Anne Cecilie Sjølie Bråthen[1], Knut Overbye[1], Jonas Kransberg[1], Øystein Sørensen[1], Pablo F. Garrido[1], Inge K. Amlien[1,2], I., Jose-Luis Alatorre-Warren[1], Athanasia M. Mowinckel[1], Emilie S. Falch[1], Maksim Slivka[1], Nikolai O. Czajkowski[3], Yunpeng Wang[3], Paulina Due-Tønnessen[4], Jennifer R. Harris[5], Didac Vidal-Pineiro[1], Anders M. Fjell[1,2], Markus H. Sneve[1].

Author affiliations

[1]Center for Lifespan Changes in Brain and Cognition, Department of Psychology, University of Oslo, Norway; [2] Computational Radiology and Artificial Intelligence, Department of Radiology and Nuclear Medicine, Oslo University Hospital, Norway; [3]Department of Psychology, University of Oslo, Norway; [4]Department of Radiology and Nuclear Medicine, Oslo University Hospital, Norway, [5]Norwegian Institute of Public Health, Norway

***Corresponding Author:** Kristine B. Walhovd, Center for Lifespan Changes in Brain and Cognition, Department of Psychology, University of Oslo, POB 1094 Blindern, 0317 Oslo, Norway, k.b.walhovd@psykologi.uio.no, +47 46824662

Author Contributions: KBW conceptualized and designed the study, did statistical analyses in R and wrote the manuscript. ACSB helped form the intervention, KEØØ did most work on designing the VR city, ACSB, KEØØ, JK, and ESF helped undertake data collection, ØS and PFG conceptualized statistical models for the intervention, DVP, JK, JLAW, AMM, ES and MS managed, post-processed and curated data, NOC, JRH, YW and AMF served as consultants to study design, YW devised zygosity analysis, PDT did radiological evaluations, DVP performed reliability analysis, MHS performed brainprint imaging analyses, all authors commented and contributed to the manuscript draft.

Competing Interest Statement: The authors have no competing interests to disclose.

Classification: Biological Sciences; Neuroscience; Cognitive Neuroscience

Keywords: cerebral cortex, fetal development, plasticity, lifespan changes, brainprints

This PDF file includes: Main Text; Figures 1 to 5; Tables 1 to 2

Abstract

Determining the timing of influences on the brain through the lifespan is a key challenge. What makes brains of individuals differ and converge? We studied effects of variation in prenatal versus experimental adult environment in twins (68 monozygotic, 35 dizygotic pairs, age 16-79 years), using birth weight discordance as proxy of prenatal environmental differences and navigation training in virtual reality as controlled adult influence. Monozygotic twins had more similar neuroanatomical fingerprints - “brainprints”- but similarity varied by birth weight discordance, especially for cortical area. Training made monozygotic brains stay similar, even with change, but caused dizygotic brains to diverge, mostly by curvature. Follow-up analyses indicated training increased white matter curvature and area. Thus, in adulthood, early life environmental difference made brains of genetically identical individuals deviate, while environmental influence still interacted with genetics at the grey-white-matter boundary. Distinct cortical features varied with early versus adult environmental differences.

Introduction

Mammals have a genetic program for corticogenesis, much of which unfolds in utero (1, 2). Cortical morphology is thus highly heritable and vulnerable to prenatal genetic and environmental perturbations (1, 3-6). Still, prominent cortical changes are normally seen throughout the human lifespan (7), and regional cortical changes have been demonstrated in response to relatively short-term interventions in adulthood (8-14). This scenario makes it a paramount challenge to determine the timing and nature of influences on the developing, adult and aging human brain.

Multiple diseases affecting mental function, both neurodevelopmental and neurodegenerative, are associated with smaller cortical volumes (15-17). Such individual differences are often ascribed to factors influencing trajectories of cortical change, and there is optimism for the possibility of improving brain health by environmental modification even in older adulthood (18-21). However, neurodevelopmental origins of variation in the brain and its function through the lifespan are acknowledged (22-25), and genetic factors in brain changes have been identified (26). These perspectives on human brain dynamics need integration (27). How and when can environmental influences, beyond genetics, change the human cerebral cortex? Here we seek to identify which features of the adult and aging cortex may be ascribed to early versus later environmental influences, by longitudinally studying systematic variation in prenatal versus adult environment in genetically identical and fraternal twins.

What is the nature of cortical characteristics that can be environmentally changed, when, and for how long? The radial unit hypothesis of cortical expansion posits that the extent and timing of developmental processes differentially impact area and other cortical features (2). Cortical area is to a greater extent determined by number of cortical columns generated in utero in the early embryonic period, whereas thickness is influenced by characteristics arising in fetal life, such as number and density of cells, but also neuronal and glial processes and synapses, peaking at later stages (2, 28). Human lifespan cortical development is remarkably different for these metrics, with area peaking during childhood, while greater age changes in thickness are seen through older age (7, 23, 29, 30). Moreover, prenatal growth has been more strongly associated with area than thickness (23-25). In contrast, intervention effects in adulthood have been shown for cortical volume and thickness (9, 10), but to our knowledge not for area or curvature. However, environmental differences during childhood maturation, including training, relate to regional differences also in cortical area (31). Thus,

environmental influences at an early stage may have especially prominent and lasting effects on cortical area. Still, later stage influences can also affect cortical morphology. Cortical volume is necessarily influenced by both thickness and area. Curvature, measures of cortical folding (32), may relate to thickness as well as area and volume. Cortical volume and curvature, then, may be shaped by both early and later environmental influences. Of note, most MRI-derived cortical measures, including area, thickness, volume and curvature, depend on the delineation of the grey-white matter boundary of the cortex, and processes affecting this, such as intracortical myelination, may take place in both gray and white matter and their interface (33-35).

What makes the brains of genetically identical individuals differ, and what make them similar? We address these questions by experimentally studying an index of brain similarity of MZ and DZ twins, "brainprints" (36-38). Brainprints are holistic representations of cortical anatomy, here calculated from 272 different features including area, thickness, volume and curvature (32, 39). We use these brainprints to systematically compare the cortices of individuals of varying genetic and environmental similarity at different ages. In our study, variance in environmental similarity at early developmental stage is indexed by extent of birth weight (BW) discordance, while in adulthood, environmental variance is experimentally induced by a novel navigation intervention utilizing true locomotion in immersive virtual reality across multiple weeks. These environmental influences are, of course, beyond age of influence, very different, and cannot be equated. However, similar influences cannot, for ethical and practical reasons be induced at fetal stage and in adulthood. We chose to use differences in birth weight and navigation training as example variables of environmental variance based on previously observed effects of both on cortical morphology (11, 23-25, 40).

Based on the heritability of cortical characteristics (4), and the fetal corticogenesis (2), we hypothesize similarity of cortical brainprints to scale strongly with genetic relatedness, with high similarity in identical twins, but attenuated by differences in fetal environment. What happens to the effects of genetic and earlier environmental influences on the brain with controlled environmental intervention in adulthood is uncharted area. At a behavioral level, it has been proposed that the effect of practice is to decrease the effect of previous environmental variation and increase the relative strength of genetic influences on performance (41). We test if this is the case at the cortical level – if brainprints of identical twins stay similar with training, relative to the brainprints of fraternal twins. We hypothesized

that brainprints would be more similar in MZ than DZ twins, but –throughout adulthood, still substantially less similar in MZ twins with larger birth weight discordance. Further, we hypothesized that navigation training would make the cortical brainprints stay similar in genetically identical relative to fraternal twins so if they change, they change in the same way in MZ, but differently in DZ, and that different cortical features may reflect the early developmental versus adult environmental differences, in accordance with the radial unit hypothesis. This will demonstrate how experimental paradigms with twins, using naturalistic variance in genetics and early environment, can be employed to ascribe variance in current cortical morphology to different life stages.

Results

We investigated adult twins (68 MZ and 35 DZ pairs, total n = 206 individuals, age range 16-79 years, mean age 37 years at first valid MRI), with varying degrees of prenatal environmental variance, as indexed by their extent of BW discordance (0-1750g). Half of the sample trained in a novel navigation intervention utilizing true locomotion in virtual reality, assessed with brain MRI, at pre- and post- 10 weeks intervention in an ABB/BAB (train-rest-rest/rest-train-rest) cross-over design (see Figure 1 and Methods and materials, Tables 1 and 2). The other half served as passive controls with the same measures. The project was designed to have both twins in a pair in the same training/rest/passive condition simultaneously. In practice, this did not invariably happen for all pairs, as described in Materials and methods, Behavioral data from the intervention, and SI. Analyses to take this into account were also performed. Participants were included in the present analysis if at least one adequate MRI scan was obtained. Anatomical brainprints from T1w and T2w scans were used to assess effects of genetic (MZ/DZ), early (BW) and later (navigation training) environmental differences on cortical characteristics. BW discordance of twins was calculated as a continuous variable, using the within-pair difference as a ratio. Effects of zygosity, BW discordance and training were analyzed using generalized additive mixed models (gamm4, R version 4.3.3). Two main models were run:

- At baseline, cortical brainprint similarity was predicted as a function of zygosity (1= MZ, 2 =DZ) + age (smooth) + sex (0=F, 1=M) + mean BW ((twin1+twin2)/2) + BW ratio (heaviest twin / lightest twin) + zygosity x BW ratio.
- Longitudinally, brainprint similarity was predicted as a function of training status (0= no-training,1=post ~10 weeks of training, 2 = post ~10 weeks of rest after training) + zygosity (1= MZ, 2 =DZ) + age (smooth) + zygosity x training status.

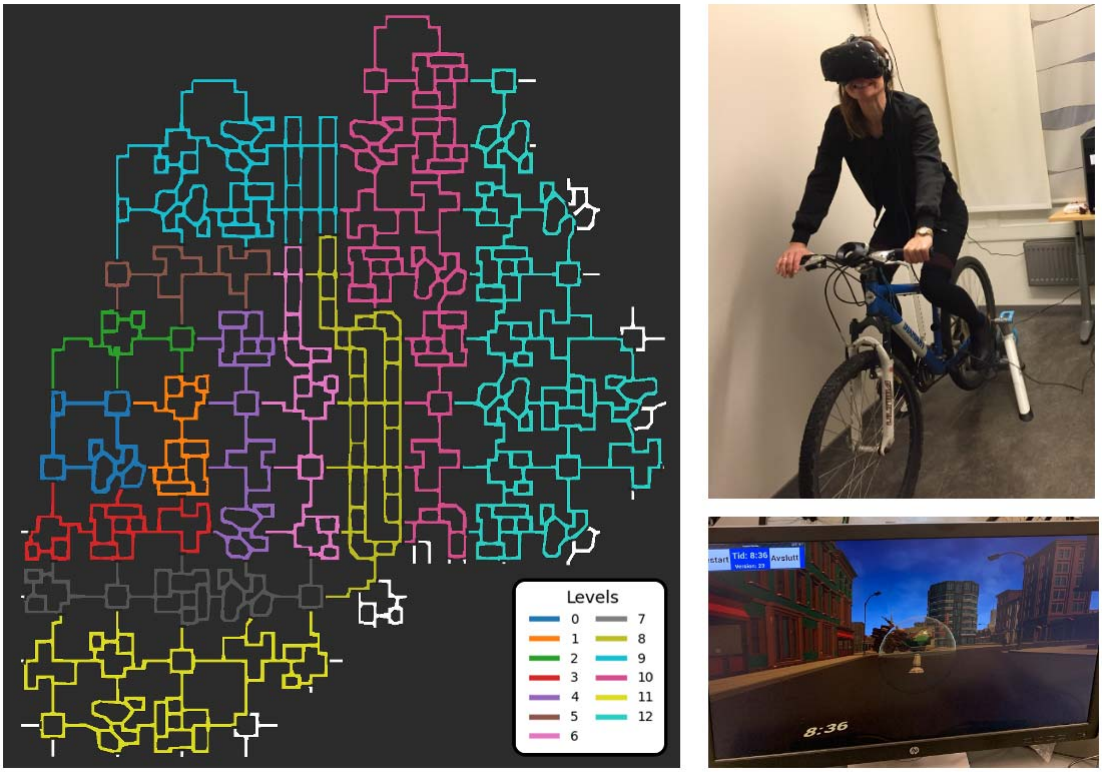

Figure 1 The virtual town Plasti City, in which the immersive VR navigation intervention took place. *Left panel: the outline of the roads, colored by level, which were opened up successively, according to participants' performance. Right panel: the cybercycle set-up in the lab. (Per request of biorxiv.org, note the picture is of the 1st author.) The screen shows what a participant sees in VR. A target is shown above the bicycle handlebars, with time passed in current session. In the homework version, the same is shown on the laptop screen.*

Baseline model: Brainprint similarity varies as a function of genetics and environmental differences in the months prior to birth

Using "brainprints" (36) from multicontrast MRI data (see Materials and methods), we observed that self-similarity was high at baseline as well as across 10 weeks. Brainprint similarity could be used for perfect identification of oneself and one´s MZ twin, and DZ-similarity was also identifiable (Figures 2A –baseline, and Figure S1 – across 10 weeks). For these analyses, MRIs before any training had commenced were used. For the baseline analysis, data were available for 101 pairs (67 MZ, 34 DZ). Since twins have identical age and sex, analyses were performed for brainprint similarity after residualizing individual brain

features on age (smooth) and sex via generalized additive models (GAMs). The "raw" brainprint similarity is shown in Figure S2.

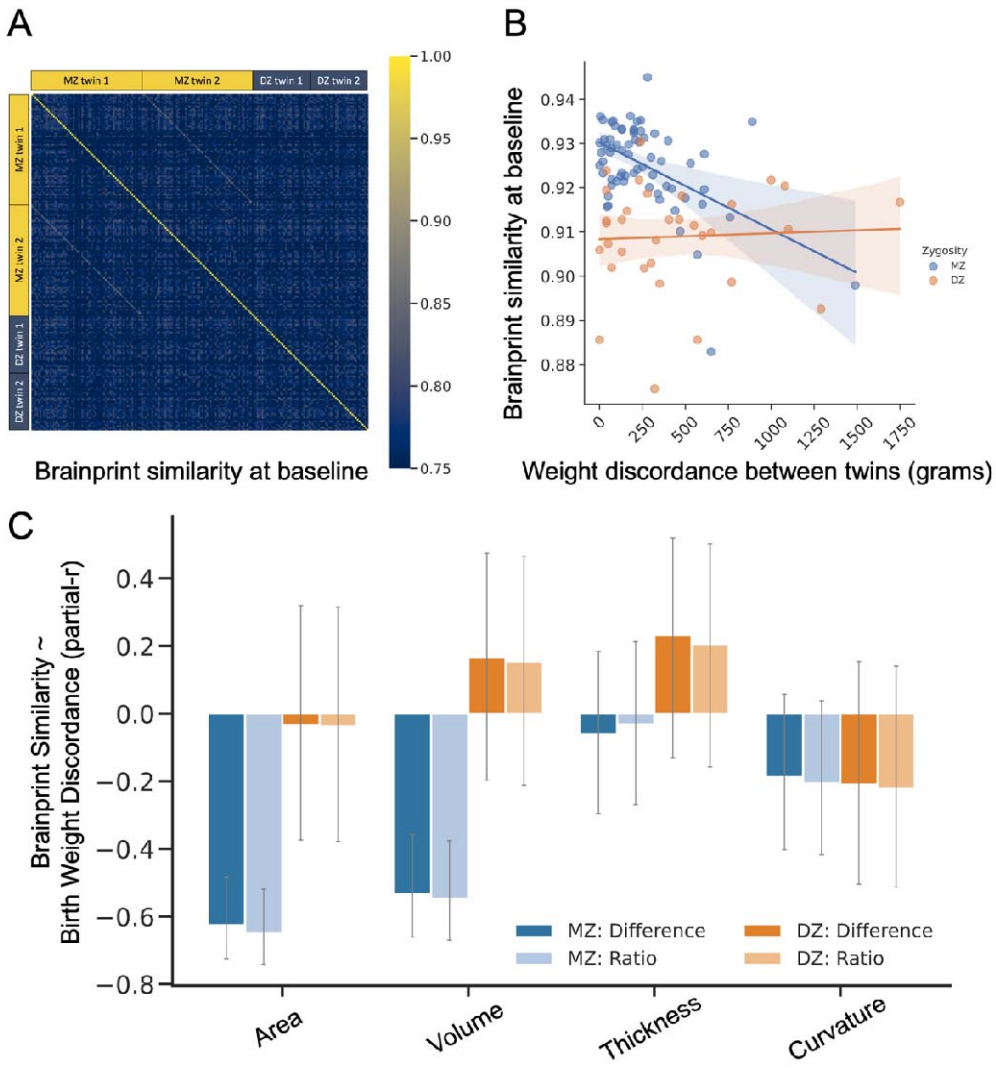

Figure 2. Brainprints in relation to genetic and environmental influence before birth

Brainprints were calculated based on 272 normalized cortical features from T1 and T2 weighted MRI scans, consisting of estimates of cortical thickness, area, volume and curvature of 68 regions. A) Pairwise similarity between the full anatomical brainprints, plotted as a function of genetic relationship. The diagonals hence represent brainprint correlations – monozygotic twins (MZ) can readily be identified from the upper left diagonals, and some, but lower, dizygotic twin (DZ) similarity is also apparent in lower right diagonals. The

individual brain features going into the brainprints were residualized for age (as a smooth function) and sex, before pairwise brainprint similarity was calculated. B) Brainprint similarity at baseline between twins varied as a function of birth weight (BW) discordance in 67 MZ pairs (blue) (r = -0.54, p < .001)*, but no such tendency was seen in 33 DZ pairs (orange). See Figure S3 for alternative operationalizations of BW discordance. C) The effects of BW discordance, whether operationalized as a ratio or absolute difference between twins in grams, were primarily driven by differences in cortical area in the MZ twins specifically, thereby impacting also cortical volume. Error bars reflect 95% CI.*

For the analysis on brainprint similarity at baseline as a function of BW discordance (Table S1; GAM formula 1), data for 100 full pairs were available (67 MZ, 33 DZ). Brainprint similarity at baseline varied as a function of zygosity (t = -4.586, p < .0001), BW ratio (t = -4.498, p <.0001), and the interaction of zygosity and BW ratio (t = 3.549, p = .0006). This interaction was due to BW ratio being negatively correlated with brainprint similarity in MZ (r = -.54, p < .001), but not in DZ twins (Figure 2B). That is, in MZ, the greater the BW difference, the less similar were the brainprints. Analysis on BW ratio effects on brainprint similarity in the MZ sample, showed that cortical area effects dominated (t = 6.748, p < .001), followed by volume (t = 5.155, p < .001), with minor and non-significant effects on curvature and thickness. For DZ, comparatively minor effects of BW difference and ratio were observed (Figure 2C).

We next plotted the feature-wise effects of BW ratio in MZ twins only (Figure 3). Of the 19 single cortical features differing significantly when false discovery rate (FDR)-corrected, nine were for area, seven for volume, two for curvature, and only one for thickness, all being in the negative direction – the greater the BW discordance, the lesser the brainprint similarity. Region-wise, effects were widespread, and found across frontal, parietal and temporal areas as well as in the insula and cingulate cortex.

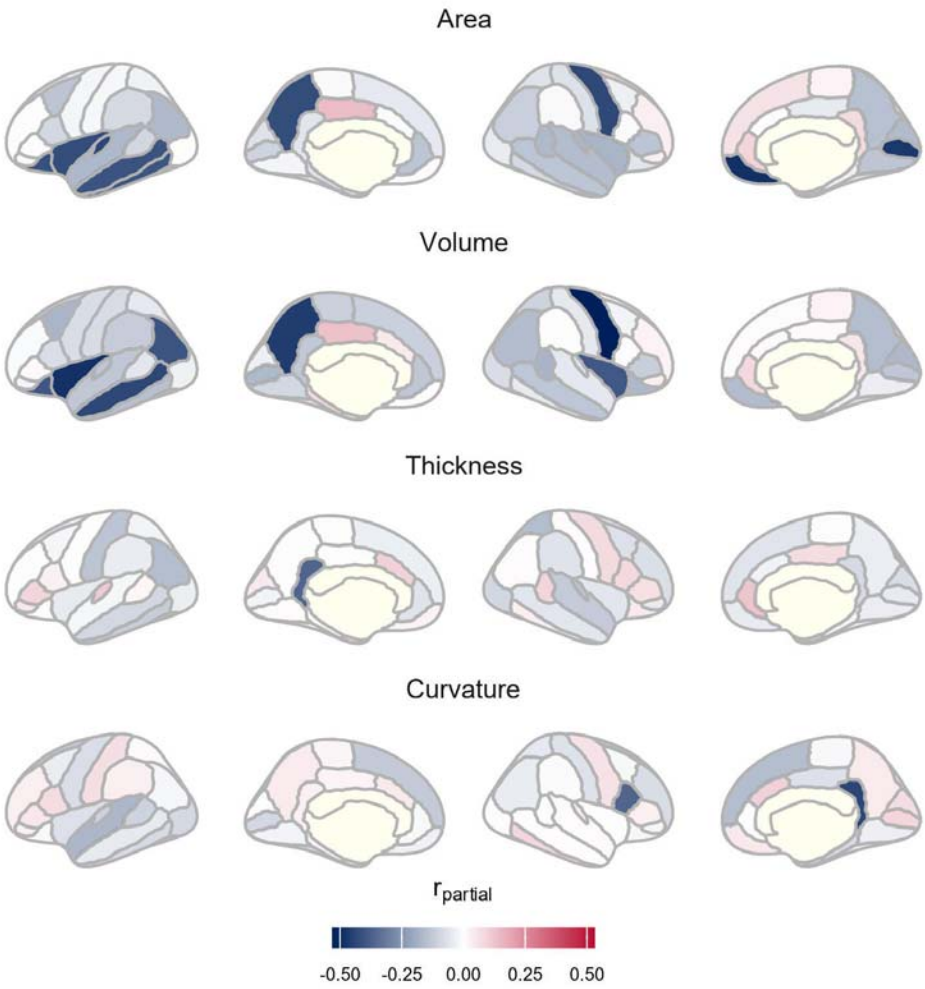

Figure 3. *Feature-wise brainprint similarity in MZ twins as a function of birthweight (BW) discordance (ratio measure). Color represents the partial correlation coefficient (r-partial) from the GAMM model, indicating the strength and direction of the association. Opaque regions are significant after FDR-correction (pFDR < .05). The four rows correspond to different feature categories (Area, Volume, Thickness, Curvature). Brain views show left and right hemispheres, lateral and medial surfaces.*

Direction of effects of early life environment detected in brainprints

To confirm, as indicated in previous studies, that lesser BW yielded lesser cortical area (23-25), and that this was driving the direction of dissimilarity in brainprints, we ran a GAMM predicting normalized summed cortical area across hemispheres at baseline MRI (n = 200) as a function of BW, age and sex, with a random intercept per twin pair (Table S1; GAMM formula 2). There was as expected a positive effect of BW on cortical area (t = 4.114, p <

.0001). This effect was somewhat attenuated but held also when adding normalized intracranial volume (ICV) as a covariate ($t = 2.448$, $p = .0153$; Table S1; GAMM formula 3). When running this GAMM on the MZ sample only ($n = 134$), positive effects of BW on area were much stronger ($t = 10.900$, $p < .0001$), in line with the zygosity x BW interaction observed in the brainprint analysis. This effect was also somewhat attenuated, but remained strong, when including ICV as an additional covariate ($t = 7.209$, $p < .0001$), and was unaffected by the inclusion of current body mass index as an additional covariate ($t = 7.147$, $p < .0001$, Table S1; GAMM formula 4). Finally, as cortical area as a metric is traditionally measured at the white matter surface, we also ran a GAMM (Table S1, formula 2) on the cortical area measured at the pial surface (see Methods). This confirmed that there were equivalent positive effects of birth weight also at the gray matter surface area ($t = 4.177$, $p <.001$), and that these were as strong also within the MZ subsample ($t = 11.070$, $p <.0001$).

Longitudinal analyses: Cortical brainprints can still be altered in adulthood in response to current environmental influence – navigation training in virtual reality

Using all data from all three time-points, a GAMM was used to predict brainprint change as a function of training status and zygosity, and the interaction of zygosity x training status (Table S1; "GAMM formula 5"). For this analysis, 484 MRI observations were available for the pairwise analyses, i.e. 242 brainprint similarity estimates, from 103 twin pairs (68 MZ, 35 DZ). In the main analyses, all twin pairs where one or both twins trained less than 2 hours or did not level up in Plasti City (i.e. remained at level 0, the baseline level, throughout training) were recoded as passive controls with training status == 0 for all measurements. A total of 100 participants had more than two hours of training and post-training MRI, of whom "complete and training-concordant" were 28 MZ and 15 DZ full pairs. (For results with complete removal of pairs from analyses rather than recoding as passive controls, see SI, Supporting results, Alternative analysis). 102 pairs had baseline measurements, either as passive controls or pre-training (training status = 0), 43 twin pairs had observations immediately post-training (training status = 1), and 21 pairs had observations also ~10 weeks after ending training (training status = 2). Significant interaction effects of training and zygosity were seen on brainprints immediately post-training ($t = -2.863$, $p = .0046$), with the brainprints of genetically identical twins staying, or even becoming relatively more, similar with training, while those of fraternal twins diverged, an effect which was attenuated ten weeks after ending training ($t = -1.519$, $p = .1300$). (Note that this effect was virtually identical and significant also when fully excluding all pairs showing discordance in training,

Supporting results, Alternative analysis.) Effects on different cortical features as well as an example of regional interaction data are shown in Figure 4. Aside from one effect on right precentral thickness, five out of six features for which the interaction of zygosity and training status was significant, were for cortical curvature.

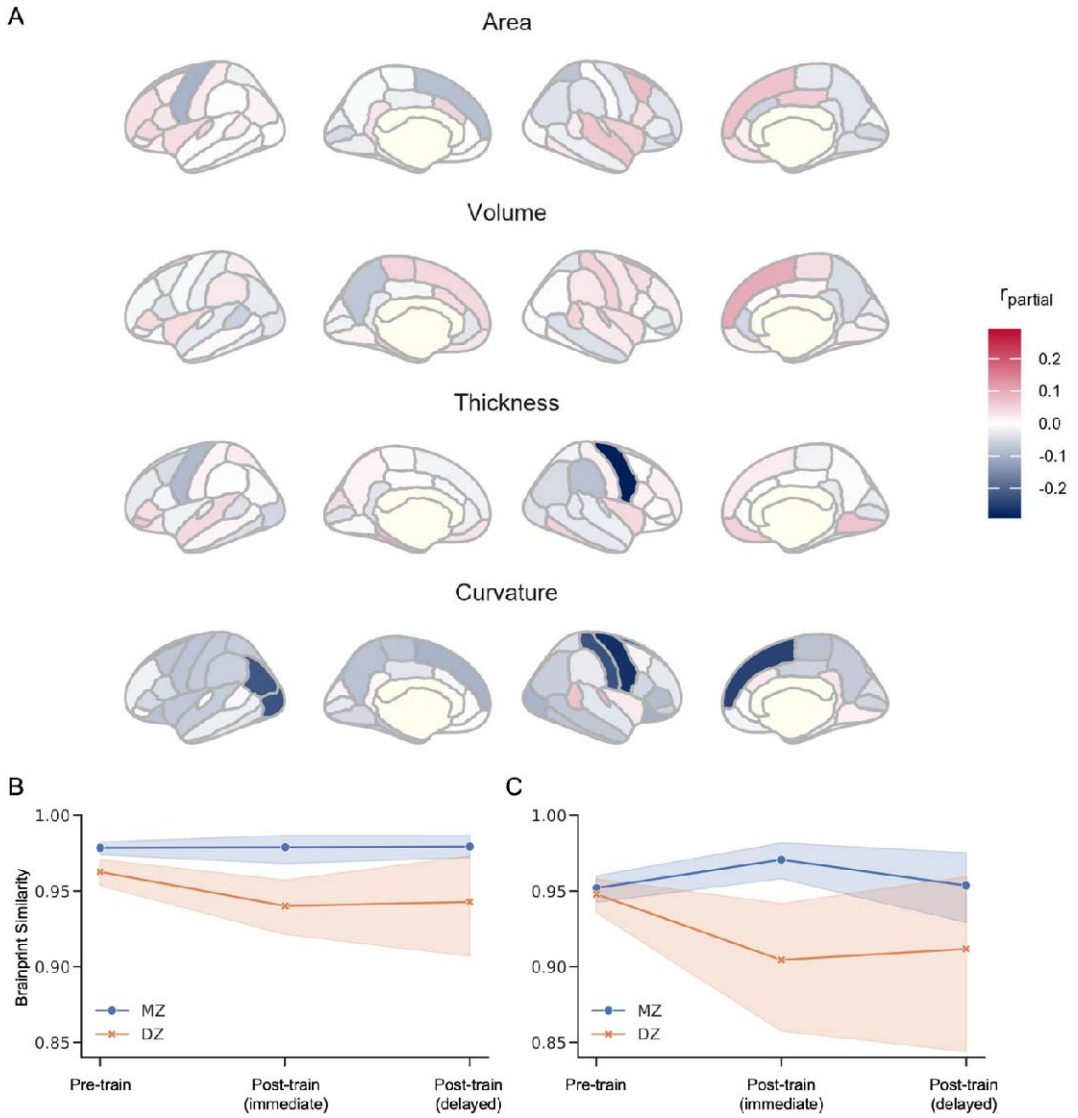

Figure 4 *The effect of training status and zygosity on brainprint similarity. A) The maps show partial correlation coefficients (r-partial) associated with the interaction between training status (immediate post-train period) and zygosity, from the GAMM model. Negative values indicate that MZ twins became more similar with training relative to DZ twins. Opaque regions indicate features surviving FDR-correction (pFDR < .05). B-C) Example interactions from the most significant features, showing how genetically identical twins (MZ) remain similar, or even become more similar, in terms of cortical features with training, whereas*

fraternal twins (DZ) become less similar in B) right precentral cortical thickness; and C) right precentral cortical curvature.

Since time between scans could differ slightly between twins, we also reran the model including the absolute age difference between twins at each session, with no change in results.

Additional analyses taking into account differences in training time and levels reached
Behavioral descriptives from the intervention (see Methods and materials, Behavioral data from the intervention) showed much variation, which again may relate to both genetic and early environmental influences. We tested whether training time discordances on average differed between MZ and DZ groups and found no significant difference (Mann-Whitney U = 195, p = .3047). Difference in level reached was however smaller for MZ than DZ twins (Mann-Whitney U = 76.5, p = .0001; mean MZ = 1.3, DZ = 3.875). The sample is smaller than ideal to analyze more fine-grained brain-behavior interactions across zygosity. However, in the MZ twins who trained and were scanned post-training, correlation analyses of the behavioral data suggested that birth weight differences relative to co-twin, moderately related to their current behavioral differences in training (twin minus twin scores). Birth weight difference correlated positively with difference in level reached (r = .30, p = .0193) as well as difference in training time (r = .36, p = .0036, df = 60), with the heavier twins training more and reaching a higher level in the navigation game. This may be suggestive of early life environment also affecting current behavioral plasticity by differences in effort invested. While the study is not well-powered to investigate fine-grained differences in brain-behavior in relation to this, two follow-up analyses were conducted to attempt to account for differences in training time and level reached in training within the pairs who trained.

We thus ran a model including a difference term for total training time within pairs (z-normalized absolute difference in training times between twins in a pair, for passive controls difference in total training time =0), i.e.: *Brainprint similarity = training status + zygosity + training time difference + s(age) + training status x training time difference + zygosity x training status* (Table s1; GAMM-formula 6). This showed that while brainprints (being less similar for DZ, t = 7.054, p < .0001) became more similar after training (immediately post-training, t = 2.229, p = .0268; n.s. after additional 10 weeks of rest), and training status still partially interacted with zygosity to make MZ more similar than DZ (training status 1 x zygosity 2: t = -1.851, p = .0655; training status2 x zygosity 2: t = -2.215, p = .0277), the

difference in training time (ns) interacted with training status (training status1 x training time difference: t = -7.512, p < .0001, n.s. after 10 weeks of rest post-training): if one twin trained more than the other, they turned less similar, i.e. there was a significant interaction of training status and training time on brainprint similarity immediately post-training. Reducing features to those derived from cortical curvature only (similarity estimated over 68 features), or to the features showing FDR corrected significant effects in the main analysis (similarity estimated over 6 features, ref. Fig.4A), interaction effects of zygosity and training status were upheld: MZ twins turned more similar immediately after training compared to DZ twins, also when controlling for training time difference within pairs (68 features: t=-3.367, p = .0009; reduced to a trend after 10 weeks: t = -1.887, p = .0605; 6 features: t=-4.701, p < .0001; after 10 weeks: ns, Table s1; GAMM-formula 6).

Finally, a GAMM was run including difference in level reached within each pair in training. *Brainprint similarity = training status + zygosity + max level difference + s(age) + training status x max level difference + zygosity x training status* (Table s1; GAMM-formula 7). There was a significant interaction of training status and level reached on brainprints immediately post-training (t = -2.555, p = .0113), indicating more similar brainprints with greater similarity in behavioral level reached. Other terms were then rendered non-significant, with the exception of a persistent effect of zygosity, with brainprints of fraternal twins being less similar (t = -6.755, p < .0001). As noted (Methods and materials, Behavioral data from the intervention), differences in level reached vary by both genetics and early environment, and thus it may not be surprising that this variable can soak up much of the variance in brainprints.

Direction of effects of training detected in brainprints

To investigate direction of training effects with increasing brainprint similarity, a GAMM (Table S1, formula 7) was run predicting global cortical curvature in the full twin pair sample as a function of training condition, with age at baseline, sex, time (since baseline) and age at baseline x time as covariates, with participant id and twin pair as random factors. In this analysis, all observations, not only pair-matched per time point, were included (n = 511). This showed a positive effect of training status on global cortical curvature (immediately post-training: t = 2.331, p = .0201, ~10 weeks post-training: t = 3.646, p = .0003). Cortical curvature is a folding measure, but is, like area, measured at the white matter surface, and can be increased with folding, but also with age and injury because of white matter atrophy (32,

42, 43). To explore potential causes of the observed curvature changes, an equivalent GAMM was run with total cortical area as the dependent variable (z-scored, n = 511).This showed a positive effect of training status on global cortical area immediately post-training (t = 2.637, p = .0086), which was not significant ~10 weeks post-training (t = 1.265, p = .2066). Given the observed effect on cortical area as traditionally measured at the white matter surface, equivalent GAMMs for mean curvature and area measured at the pial surface were run to further assessing whether the observed changes extended to the entire cortical mantle (see Methods). However, there were no significant or near-significant effects of training on these pial measures. For specification of effects of all terms in these GAMMS, see SI, Supporting results. See the feature-wise effects of training in the full twin pair sample in Figure S4(GAMM (Table S1, formula 7). Note that inferential statistics were not interpreted for this analysis; the plot is provided solely for illustrative and transparency purposes. Collectively, the findings are suggestive that training served to expand the white matter specifically, acting on the gray-white matter boundary, and not the pial cortical gray matter characteristics.

Distinct features of the cortex vary as a function of example environmental influences in early development versus adulthood

Comparing the distributions of cortical features for which our example early (birth weight) versus later (navigation training) environmental influences interact with genetic similarity, a dissociation emerges: Birth weight discordance yielded effects dominated by cortical area, thereby affecting also volume (Figure 4A), whereas training effects in adulthood were seen chiefly for cortical curvature, with some more restricted effect also on thickness. To visualize the varying gene x environment effects on the cortex, we compared brain similarity as a function of environmental status (birth weight, training) + zygosity + age (smooth) + zygosity x environmental status (Figure 5). Note that for birth weight ratio, we also add mean birth weight and sex to the equation, as this may affect the birth weight discordance association with the cortical features cross-sectionally.

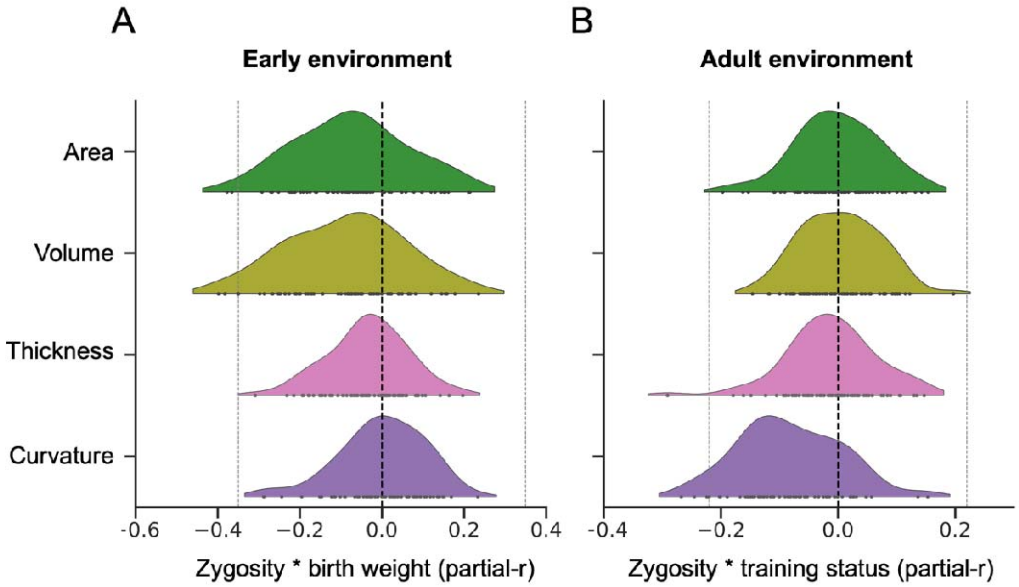

Figure 5 *The differing distributions of gene-environment associations for cortical features with the early versus adult environmental influences. The x-axes represent partial correlation coefficients from GAMM models, reflecting the strength and direction of the interaction between zygosity and birth weight ratio (early environment, panel A), and zygosity and training status (adult environment, panel B), on brainprint similarity. To summarize differences in the distribution of these region-wise effects across feature categories, Kruskal-Wallis tests were performed (Early environment: H = 20.7, p = .0001; Adult environment: H = 41.7, p < .0001). Dunn's post-hoc tests (Bonferroni-corrected, only showing significant effects) indicated differences between Area and Curvature (p = .001/.0001), and Volume and Curvature (p = .0003/<.0001), with additional differences between Thickness and Curvature in the adult environment (p = .0001). Individual datapoints represent partial correlation coefficients for individual cortical regions.*

Discussion

Utilizing a twin design, the results demonstrate that genetic, and early and later environmental influences on cortical anatomy can be teased apart. While early environmental influences had lasting effects, later influences, indexed by navigation training, caused the cortical anatomy of genetically identical twins to stay similar, or even converge, relative to that of fraternal twins, which diverged. We also show a double dissociation between these select early versus current environmental influences interacting with genetics on specific cortical characteristics,

demonstrating that features of the cortex vary greatly in amenability to change with different types of influences. In sum, these findings draw a picture of the early life environmental influences being persistent on cortical area, as seen both at the white-gray matter interface and at the pial surface. Cortical area and curvature, as measured at the white matter surface, still appear amenable to change at later stages, while this plasticity was not traceable in global measures at the pial surface. There are no conceivable environmental influences in adulthood equivalent to those affecting prenatal growth. Thus, we cannot equate impact of the early and later environmental influences with potential for change at different life stages. The present findings suggest that these early life influences indexed by birth weight, whatever their nature, persistently shape cortical area and the gray matter surface through life, both independently of genetics and interacting with it. In contrast, plastic changes at the cortical white gray-interface, here interacting with genetics, may take place with cognitive training in adulthood.

The persistent effect of early environment on brainprint similarity of genetically identical twins aligns with studies of effects of normal variance in prenatal growth along the lifespan on select cortical characteristics. For instance, we have previously shown that birth weight relates to cortical volume and area in a broad and topographically stable way across the lifespan (25). Other studies have also shown BW discordance to have enduring effects on the brains of MZ twins at later developmental stages (40, 44, 45), though not invariably (46). For cortical morphology, two studies have reported effects of BW discordance on cortical area and volume, but one study was restricted to MZ twins (45). The other study, while finding prominent cortical effects of birth weight, did not find statistical interactions with zygosity (40), thus concluding that birth weight correlates within DZ twins were not significantly different from those observed within MZ twins.

The current study, however, indicates substantially stronger effects of birth weight variations within MZ twins, where the environmental source of variance in birth weight has a greater effect on cortical characteristics, than birth weight variation as influenced also by genetics. It should be noted that both previous studies on cortical morphology in twins (40, 45) used a different methodology for delineating cortical area, thickness and volume (CIVET; http://www.bic.mni.mcgill.ca/ServicesSoftware/CIVET). The current study focuses on these cortical metrics in addition to curvature, using FreeSurfer (FS) (https://surfer.nmr.mgh.harvard.edu/) and brainprints (36), and this may have influenced the

results (35). We previously, using FS, showed an age-invariant effect of birth weight discordance on cortical area in genetically identical twins, including a subsample of the current sample (25). The present findings reveal the robustness of the environmental effect in making the multi-feature cortical brainprints (36) diverge in genetically identical relative to fraternal twins across varying ages. Hence, while the relationship between birth weight and cortical characteristics in DZ twins and the population at large likely partly reflects variation in genetically determined body and brain size, the variance observed in MZ twins reflects environmental effects on early brain development. The enduring effect on their cortical brainprints through adulthood is in correspondence with other evidence that select processes in cortical development exclusively happen before birth. For instance, neurogenesis takes place almost only in fetal development, even though synaptogenesis, synaptic remodeling and myelination are known to be protracted processes long after infancy (2, 28, 47-51). Humans are born with almost all cortical neurons they will have through life, and neuronal migration and differentiation are also defined early (2). Factors that affect placental function and uterine or umbilical blood flow on a chronic basis may lead to restricted fetal growth, including brain growth, with stable effects across years (25, 52), and especially strong effects on cortical area at white and pial surfaces, in accordance with the radial unit hypothesis (2).

While it has been observed that behavioral heritability can be increased with training (41, 53), the present findings additionally indicate that induction of similar environments by training in adulthood can make the brains of genetically identical individuals stay similar, or even to some extent converge, as if they change, they change the same. We note that this interaction of zygosity and training is driven also largely by fraternal twins becoming less similar with training. Navigation training may be a suitable paradigm for inducing such changes, as the ability to navigate shows wide variability that appears to relate to both genetic and environmental differences (54, 55), and effects of navigation training on brain structural characteristics have also previously been demonstrated (11, 56). The currently observed gene-environment interaction on cortical brainprints thus aligns with a vast amount of evidence from behavioral studies: Since genes work through environment, effects of genetic variance will become more evident given similar environmental opportunity for the different genetic influences to unfold (41, 53, 57, 58). While genetically different individuals then will become more different, genetically identical individuals will stay the same or may even become more similar, with increasing environmental similarity. The observed interaction of zygosity and training on cortical brainprints indicate a neural substrate for this gene-environment

interaction. This divergence of the brainprints of fraternal relative to identical twins with training, is in line with the observation that behavioral training serves to increase absolute variance, i.e. interventions cause a wider distribution of individual differences, even if the relative proportion explained by genetics increases (53). While the direction of effects of both differences in birth weight and training were positive for cortical area and curvature, respectively, the curvature effect of training in adulthood is much smaller, and may in part also reflect subtle changes in underlying white matter surface. This is indicated by increase in total white matter area, but not in pial cortical area, with training. Curvature as a metric associates with gyrification. Rapid growth of intracortical neuropil, addition of glial cells, and enlargement of subcortical white matter in primates are the primary forces responsible for the post-neurogenic expansion of the cortical surface and formation of gyri during fetal development (59). The same mechanisms cannot be assumed to underlie changes in curvature in adulthood, especially as changes in curvature here appear to occur in the absence of changes in pial curvature and area. However, changes in e.g. intracortical myelination and synaptic density may be at play in changes in curvature as measured at the white matter surface, white matter area and cortical thickness changes in adulthood (33, 34). Additional studies and parameters are required to fully understand the neurobiological mechanisms underlying these effects.

The environmental influences studied here, namely fetal growth conditions and immersive navigation training, are as noted very different, beyond age of influence, and cannot in any way be equated. Thus, beyond studying age of influence, we are studying type of influence. However, similar influences cannot, for ethical and practical reasons be induced at fetal and adult stage, and we need to be aware of the strength of human fetal and early life influences relative to anything we observe in adulthood (27). One reason for this, is not only the timing of neural development, such as seen for corticogenesis (2), but that the effects of early life influences are being carried out through numerous years and interactions with the environment (60), while any influences we inflict in adulthood are bound to work over a much shorter time period. This is seen for instance, in the relations of both genetics and early life environment with behavioral measures from the current intervention: Genetically identical twins tended to reach more similar levels of performance, but the heavier twin tended to attain a higher level of performance, training more. Observed in a restricted experimental setting, even though designed to have ecological validity, such relations may be only weakly suggestive of the real-world effects taking place across decades.

Cortical representations as here captured in brainprints show the extent of individuality of human brains (36, 37), and can be used to decompose how and when this individuality may unfold, based on genetic and environmental variance trough the life course. As pointed out by Sidman and Rakic, ontogenetic mechanisms must be comprehended in terms of the prolonged time of maturation, large size and other properties peculiar to the human brain (61). Luckily, the long human lifespan allows a temporal resolution whereby we can truly observe the persistence of early life influences on specific cortical features, coupled with preserved plasticity of others. Further understanding of such fundamental concepts should thus come also from human studies, rather than primarily non-primate species (61, 62). Experimental neuroimaging designs including MZ and DZ twins can be used to advance our understanding of what works when and for how long on the human brain. The current paradigm and results suggest a model for how and when effects of example early and later life influences on the human brain can be modified and studied across the human lifespan.

Materials and methods

Sample

The project was approved by the Regional Committee for Medical Research Ethics, South Norway, and all participants gave written informed consent. The full co-twin MRI sample reported on here, constitutes a subsample of the full Set-to-change study sample, where individuals part of full twin pairs with MRI data for both twins, comprised 206 individuals (age range 16-79 years at baseline), of whom 136 MZ and 70 DZ twins. For this sample, 4 sets of MRI data for participants scanned at wave 1 were excluded due to scan artefacts (2) or lost due to human error (2), but these participants had MRI data at waves 2 and 3, and were included in analyses where appropriate. The majority of the present sample (n = 186; 90%) was recruited through the Norwegian Twin Registry (NTR) (63), based on availability of registry data for birth weight of both twins in pairs. Because the Norwegian Institute of Public Health, which the NTR is part of, could not resume recruiting for a prolonged period following additional task burden related to the COVID-19 pandemic, a minority of the sample (n = 20) was recruited through social media while awaiting capacity. Only same-sex pairs were recruited. For the majority of the sample (n = 186), zygosity information was retrieved from the National Twin Registry, while for ten pairs, this information was retrieved by current questionnaire assessment, and for the majority of the sample, DNA was also retrieved from either saliva or buccal swabs (n = 158), in all cases confirming the NTR zygosity information.

(For details on determination of zygosity based on DNA, see SI, Study design and sample, Genotyping.). See Table 1 and details below for a description of the sample characteristics.

Participants were recruited to be healthy, community-dwelling volunteers, without particular worries about their cognitive function or diseases known to affect central nervous system functioning. However, to be able to recruit full pairs, and given the interest in possible early biomedical risk and discordance of variables among twins, a lenient threshold for inclusion was applied. Thus, twins were not excluded based on scores for cognitive functioning, but twins above 40 years of age were required to score a minimum of 25 on the Mini Mental Status Examination (MMSE). Use of blood pressure medications and previous treatment for medical conditions were not exclusion criteria (see SI for details). In the broader Set-to-change study, 227 individuals were included, and 219 underwent MRI. All research MRI data for one participant was unfortunately lost due to human error. A radiologist evaluated scans included for clinical purposes (see below), and data for 1 participant was excluded due to a clinical finding. For the remaining MRI sample (n = 217) there were 11 cases where valid MRI data were only available for one twin, and these were excluded from the present analyses.

	Full co-twin MRI sample (140F/66M, n = 206)			**MZ twins (94F/42M, n = 136)**			**DZ twins (46F/24M, n = 70)**		
	M	**SD**	**Range**	**M**	**SD**	**Range**	**M**	**SD**	**Range**
Age	37.0	16.9	16.2-78.6	37.8	16.5	16.2-78.6	35.3	17.5	16.5-76.6
BW	2581	557	700-3900	2531	575	700-3900	2679	508	1450-3770
BW Disc.	0	455	+/-1750	0	363	+/-1490	1.7	594	+/-1750
Education	15.8	2.7	10-25	15.8	2.6	10-22	15.8	2.8	10-25
MMSE	28.7	1.1	25-30	28.8	1.0	25-30	28.7	1.3	26-30
IQ	109	12.2	63-144	109	11.9	63-136	110	12.7	70-144

Table 1. Descriptives of the full MRI sample and of the monozygotic (MZ) and dizygotic (DZ) twin subsamples at MRI time point 1.

Age and education are given in years, birth weight (BW) and birth weight discordance (disc.) in grams. Mini Mental Status Examination (MMSE)(64) scores are given for twins above 40 years of age at visit. IQ scores are from Wechsler Abbreviated scales of Intelligence (WASI)(65). Missing values: BW:1, BW discordance: 2, Education:1, MMSE: 3, WASI: 4.

Birth weight measures

For all participants recruited through the Norwegian Twin Registry (NTR) born 1967 or later, birth weight information was obtained from the Medical Birth Registry of Norway (MBRN), which is a national health registry containing information about all births. MBRN birth weight info was obtained for 152 participants. For participants born before 1967, NTR records of self-reported birth weight were used from 1) an earlier questionnaire survey (Q1) conducted 1979–1982 (66) (n = 32, including for one participant, co-twin-report from this survey), or, 2) self-reports collected in 2014 by NTR as part of the twin study Social Factors and Health (n =2). For those not recruited through NTR, current self-report was used (n = 19), but in one case, such self-report was missing. A high reliability of self-reported BW over time has been found in broader NTR samples (67). Birth weight discordance of twins was calculated as a continuous variable, where the difference within-pair in grams yielded a negative value for the lighter and a positive value for the heavier twin. A ratio score for birth weight (twin/twin) was used for discordance analyses on brainprints.

The intervention

All participants were offered to partake in follow-up assessments, as well as a navigational training intervention, being immersed in virtual reality (VR) in our lab and on laptops at home, searching for target objects and performing retrospective and prospective memory and time tracking tasks in a virtual town called Plasti City. Plasti City covers approximately 5 km^2, and sequential segments (levels, 0-12) were opened up automatically according to participant navigation performance. Illustrations of the city with the different levels and basic navigation task are shown in Figure 1, and the distribution of all navigation targets is shown in Figure S6. In addition to navigating to targets, participants got various retrospective, prospective and time tracking tasks as the training progressed (see SI, Cybercycle training program.**)**. Twins accepting the training invitation were randomly assigned to start with either a training (A) or rest (B) condition. After 10 weeks, repeated scans and cognitive assessments were undertaken, and participants were to switch conditions (A-B/B-A). After another 10 weeks, scans and cognitive assessments were again repeated (see Table 2). Similarly, participants not training were invited for repeated scans and cognitive assessments at 10 week intervals. While the intention was to schedule assessments within 11-12 week intervals, due to COVID-19-related lockdown and prolonged restrictions and practical difficulties following these (see SI, Study design and sample, Data collection), the actual intervals varied more. Mean interval between wave 1 and 2 assessment was 0.22 years (SD: 0.05, range: 0.13-0.62 years), and mean interval between wave 1 and 3 assessment was 0.45 years (SD: 0.08, range:

0.38-0.82 years). Mean interval between pre- and post-train visits was 0.21 yrs (range 0.17-0.26 years), while mean interval between post-train and post-rest-after-training visits was 0.24 (range 0.18-0.59). In cases of delays in scan times, participants training were encouraged to keep training.

MRI observations	**Wave 1**	**Wave 2**	**Wave 3**
Start train (A/B/B)	68	53	50
Start rest (B/A/B)	55	54	47
Passive control (B/B/B)	80	58	46
Total n	203	165	143

Table 2 Distribution of MRI observations (n = 511) for trainers and passive controls across waves. *MRIs immediately post-training period (n = 100) are denoted by Start train observations for wave 2, and Start rest observations for wave 3. There are 50 additional observations after ending training and resting for ~10 weeks, denoted by Start train observations for wave 3.*

118 participants in the current sample accepted to enter into the training intervention. Participants received instructions and general training in VR, first only adjusting to immersive VR with the VR goggles, before being given the task of navigating in Plasti City, looking for targets. Only time spent actively navigating in search of given targets in Plasti City was counted as training time. Based on this training time estimate, 18 participants, 14 of whom had longitudinal MRI, spent less than two hours actively moving training towards reaching targets in the city, and were in categorical analyses included as passive controls at later time points.

Behavioral data from the intervention

For the remaining 100 participants with more than two hours of training and MRIs post-training, mean training time was 14.64 hours, but time spent training varied much, ranging from 2.05 to 55.13 hours (SD: 11.04 hours). An average of 5.48 hours of the training time was spent in immersive VR (SD: 2.86 hours; range: 0.28 to 14.14 hours). On average, level reached was 6.88 (range: 1-12, SD: 3.26), and mean number of targets reached was 373.8 (range 76-921, SD: 175). Total time spent training correlated positively with number of targets reached ($r = .82$, $p < .0001$), and also with level reached ($r = .52$, $p < .001$), but not with mean deviance from shortest path ($r = .09$, $p = .3656$). The latter may be due to older

participants spending more time training (correlation of visit age and training time, r = .60), but still having greater mean deviance from shortest path (r = .50, p <.0001.) The deviance from shortest path is calculated by the difference between the participant's path and the shortest path. For additional details, see SI, Study design and sample, Data collection and Cybercycle training program. Due to the variation, brainprint analyses including training times as well as level reached as dimensional variables were also conducted.

MRI acquisition and post-processing

Imaging data was acquired using a 32-channel head coil on a 3T MRI scanner (Prisma, Siemens, Germany) at Rikshospitalet, Oslo University Hospital. Relevant for brainprint analyses were: 1) T1-weighted MPRAGE with 208 sagittal slices (TR = 2400 ms, TE = 2.22 ms, TI = 1000 ms, flip angle = 8°, matrix = 300×320×208, voxel size = 0.8×0.8×0.8 mm, FOV = 240×256 mm, iPAT = 2); and 2) T2-weighted SPACE images with 208 sagittal slices (TR = 3200 ms, TE = 5.63 ms, matrix = 320×300×208, voxel size = 0.8×0.8×0.8 mm, FOV = 256×240 mm, iPAT = 2). Both sequences were acquired with Prescan Normalize enabled to standardize coil sensitivity profiles. These sequences are identical to those used in the HCP phase 1b Lifespan pilot (https://www.humanconnectome.org/study-hcp-lifespan-pilot/phase1b-pilot-parameters).

Structural data from each wave were first processed using FreeSurfer's (v.7.3.2) default cross-sectional recon-all pipeline with the optional parameters --t2pial and --hires. The --t2pial parameter uses the auxiliary T2-weighted sequence to refine pial surface placement, while --hires processes the data at its native 0.8 mm isotropic resolution for enhanced surface detail. To further optimize reconstruction, a set of "expert-options" were used. This included the critical PlaceMMPialSurf fix (--mm_min_inside 50 --mm_max_inside 200 --mm_min_outside 10 --mm_max_outside 50) to address reported pial surface misplacements, and a pial surface placement enhancement in the inferior frontal area near the putamen (WhitePreAparc --rip-bg-no-annot). Additional fine-tuning options, as outlined in the FreeSurfer v7.3.2 post-release notes https://surfer.nmr.mgh.harvard.edu/fswiki/ReleaseNotes were also incorporated.

Base templates for longitudinal processing were created using FreeSurfer's recon-all -base command. For participants undergoing training (ABB and BAB groups), templates were

constructed using imaging data from sessions immediately before and after the intervention. This approach prevented systematic biases in the template towards either the pre-training or post-training phases, ensuring a balanced representation of both phases. For passive controls, who had no intervention, templates were created using MRI data from either sessions 1 and 2 or sessions 2 and 3, with the two variants balanced by age and sex to account for potential session-specific variability. For the subset of passive controls with only one session, the base template was constructed from the single time point, ensuring consistent resampling and interpolation across all participants.

Finally, longitudinal processing was performed using FreeSurfer's recon-all -long command. Each cross-sectional session was aligned to the participant-specific base template to ensure consistent registration and surface placement across time points. The T2w image was consistently included with -T2pial flags to refine pial surface placement, and all processing was conducted at the native 0.8 mm isotropic resolution via the -hires option.

When intracranial volume was used as a covariate in analyses, this was Total Intracranial Volume from Sequence Adaptive Multimodal Segmentation (SAMSEG) (68, 69).

Cortical morphology measures

For the FreeSurfer brainprints, cortical area, thickness, volume, and curvature were calculated for each of the 68 cortical regions defined by the Desikan-Killiany atlas (39). The definitions of area, thickness and volume followed FreeSurfer's standard approach: Cortical area was measured as the total surface area at the white surface (inner boundary of the cortical gray matter), cortical thickness as the mean cortical thickness between corresponding vertices on the white and pial surfaces, and cortical volume using a surface-based method where the space between the white and pial surfaces was divided into tetrahedra for precise volume estimation.

Cortical curvature was computed as the integrated rectified mean curvature over each region, capturing the total amount of cortical folding irrespective of fold direction. While area and curvature were originally defined on the white surface, control analyses also estimated mean curvature and surface area at the pial surface to investigate whether effects observed at the white surface might reflect changes in the underlying white matter rather than cortical gray matter.

While comparable approaches using the above cortical morphology measures for individual characterization have also included FreeSurfer's estimates of sulcal depth (70), this measure is normalized within each session, making it a relative metric specific to individual scans (71). As a result, sulcal depth values derived from Freesurfer are not directly comparable across time points and thus not suitable to investigate changes due to interventions.

Brainprint analyses

Brainprints were constructed for each participant-session by extracting the four morphological measures of interest—cortical area, thickness, volume, and curvature—for each of the 68 regions in the DK-atlas, resulting in a vector of 272 values representing cortical morphology. Note that while the current approach is inspired by Wachinger et al.´s "BrainPrint"/shapeDNA methods (37), we here use the term "brainprint" in a generic fashion. To compare brainprints within individuals over time or between individuals, we used the inverse of the mean relative difference as a similarity metric (Formula 1). This measure calculates the relative difference between corresponding features across brainprints, normalized by their average, and expresses the result as 1 - *Mean Relative Difference*. Values closer to 1 indicate higher similarity. The mean relative difference does not require features to be on the same scale (unlike alternative similarity measures such as cosine or Euclidean similarity), making it suitable for the heterogeneous brainprint measures. It can also be applied to reduced brainprints and even single features, enabling the targeted analyses presented here.

However, one limitation of this measure is its sensitivity to differences in brain size, particularly for features such as cortical area and volume, where individuals with similar brain sizes (e.g., same sex and age) may appear more similar. To account for this, non-twin comparisons included additional analyses with sex and age regressed out using Gaussian additive models with age as a smooth term. Full brainprint analyses were also repeated using cosine similarity as an alternative metric, which is scale-invariant and unaffected by brain size differences (see Figure S5). For twin comparisons (monozygotic and same-sex dizygotic), the mean relative difference metric was used without regressing out sex or age, as these analyses inherently controlled for these variables.

$$M = mean\left(\left|(x_k - y_k)/\left((x_k + y_k)/2\right)\right|\right)_{(k=1)}^{F}$$

Formula 1: Mean of the relative differences between corresponding features x_k *and* y_k*, normalized by their average, across all features* k *from 1 to* F*.* x *and* y *can represent brainprints from the same individual over two different sessions or from different individuals. Brainprint similarity equals the inverse of* M*.*

Leveraging twin pairs with two passive scans (N = 30), we observed that brainprint similarity showed high precision and sensitivity to experimental manipulation (see SI and Figure S7)

Acknowledgements

We sincerely thank all twins for their time and engagement in the study and for contributing to all the respective data sources. Data used were in part obtained through the Norwegian Twin Registry (NTR) and the Medical Birth Registry (MBRN) of Norway. We are grateful to NTR for recruiting the twins and providing data from their surveys as well as from MBRN. We thank the many research assistants who have been assisting with the training and testing, and Irantzu Anzar Martinez de Lagran for performing zygosity analysis. We are grateful to Martin Lövdén for commenting on the manuscript. This study was funded by ERC grant 771375 to and Research Council of Norway (RCN) grants to KBW. The ERC and RCN had no role in the design and conduct of this specific study.

Conflict of Interest Disclosures: The authors have no conflicts of interest to disclose.

Data Availability:

The LCBC dataset has restricted access, requests can be made to the corresponding author, and some of the data can be made available given appropriate ethical and data protection approvals. However, the registry data on birth weight connected to this sample are not shareable by the authors, as these data are owned by the Medical Birth Registry of Norway https://www.fhi.no/en/hn/health-registries/medical-birth-registry-of-norway/medical-birth-registry-of-norway/ , and the Norwegian Twin Registry https://www.fhi.no/en/more/health-studies/norwegian-twin-registry/ so that any access to data must be approved by them. The code used for main analyses can be accessed here https://github.com/LCBC-UiO/Set-to-change

References

1. K. L. Grasby *et al.*, The genetic architecture of the human cerebral cortex. *Science* **367** (2020).
2. P. Rakic, Specification of cerebral cortical areas. *Science* **241**, 170-176 (1988).
3. R. S. Desikan, A. J. Barkovich, Malformations of cortical development. *Ann Neurol* **80**, 797-810 (2016).
4. L. T. Eyler *et al.*, A comparison of heritability maps of cortical surface area and thickness and the influence of adjustment for whole brain measures: a magnetic resonance imaging twin study. *Twin Res Hum Genet* **15**, 304-314 (2012).
5. A. F. Alexander-Bloch *et al.*, Imaging local genetic influences on cortical folding. *Proceedings of the National Academy of Sciences of the United States of America* **117**, 7430-7436 (2020).
6. W. E. Snyder *et al.*, A bimodal taxonomy of adult human brain sulcal morphology related to timing of fetal sulcation and trans-sulcal gene expression gradients. *Neuron* 10.1016/j.neuron.2024.07.023 (2024).
7. A. B. Storsve *et al.*, Differential longitudinal changes in cortical thickness, surface area and volume across the adult life span: regions of accelerating and decelerating change. *The Journal of neuroscience : the official journal of the Society for Neuroscience* **34**, 8488-8498 (2014).
8. B. Draganski *et al.*, Neuroplasticity: changes in grey matter induced by training. *Nature* **427**, 311-312 (2004).
9. A. Engvig *et al.*, Effects of memory training on cortical thickness in the elderly. *Neuroimage* **52**, 1667-1676 (2010).
10. A. Engvig *et al.*, Effects of cognitive training on gray matter volumes in memory clinic patients with subjective memory impairment. *Journal of Alzheimer's disease : JAD* **41**, 779-791 (2014).
11. E. Wenger *et al.*, Cortical thickness changes following spatial navigation training in adulthood and aging. *Neuroimage* **59**, 3389-3397 (2012).
12. E. Wenger, C. Brozzoli, U. Lindenberger, M. Lovden, Expansion and Renormalization of Human Brain Structure During Skill Acquisition. *Trends in cognitive sciences* **21**, 930-939 (2017).
13. E. Wenger *et al.*, Repeated Structural Imaging Reveals Nonlinear Progression of Experience-Dependent Volume Changes in Human Motor Cortex. *Cereb Cortex* **27**, 2911-2925 (2017).
14. G. Olivo *et al.*, Estimated gray matter volume rapidly changes after a short motor task. *Cereb Cortex* **32**, 4356-4369 (2022).
15. L. M. Federmann *et al.*, Associations between antagonistic SNPs for neuropsychiatric disorders and human brain structure. *Transl Psychiatry* **14**, 406 (2024).
16. N. V. Radonjic *et al.*, Structural brain imaging studies offer clues about the effects of the shared genetic etiology among neuropsychiatric disorders. *Mol Psychiatry* **26**, 2101-2110 (2021).
17. P. M. Thompson *et al.*, ENIGMA and global neuroscience: A decade of large-scale studies of the brain in health and disease across more than 40 countries. *Transl Psychiatry* **10**, 100 (2020).
18. WHO, *Risk reduction of cognitive decline and dementia: WHO guidelines* (World Health Organization, Geneva, 2019).
19. G. Livingston *et al.*, Dementia prevention, intervention, and care: 2024 report of the Lancet standing Commission. *Lancet* **404**, 572-628 (2024).

20. J. Manuello *et al.*, The effects of genetic and modifiable risk factors on brain regions vulnerable to ageing and disease. *Nat Commun* **15**, 2576 (2024).
21. T. Shimizu *et al.*, Oligodendrocyte dynamics dictate cognitive performance outcomes of working memory training in mice. *Nat Commun* **14**, 6499 (2023).
22. E. Wheater *et al.*, Birth weight is associated with brain tissue volumes seven decades later but not with MRI markers of brain ageing. *Neuroimage Clin* **31**, 102776 (2021).
23. K. B. Walhovd *et al.*, Neurodevelopmental origins of lifespan changes in brain and cognition. *Proceedings of the National Academy of Sciences of the United States of America* **113**, 9357-9362 (2016).
24. K. B. Walhovd *et al.*, Long-term influence of normal variation in neonatal characteristics on human brain development. *Proceedings of the National Academy of Sciences of the United States of America* **109**, 20089-20094 (2012).
25. K. B. Walhovd *et al.*, Fetal influence on the human brain through the lifespan. *Elife* **12** (2024).
26. R. M. Brouwer *et al.*, Genetic influences on individual differences in longitudinal changes in global and subcortical brain volumes: Results of the ENIGMA plasticity working group. *Hum Brain Mapp* **38**, 4444-4458 (2017).
27. K. B. Walhovd, M. Lovden, A. M. Fjell, Timing of lifespan influences on brain and cognition. *Trends in cognitive sciences* **27**, 901-915 (2023).
28. P. R. Huttenlocher, Synaptic density in human frontal cortex - developmental changes and effects of aging. *Brain research* **163**, 195-205 (1979).
29. L. J. Hogstrom, L. T. Westlye, K. B. Walhovd, A. M. Fjell, The structure of the cerebral cortex across adult life: age-related patterns of surface area, thickness, and gyrification. *Cereb Cortex* **23**, 2521-2530 (2013).
30. A. M. Fjell *et al.*, Continuity and Discontinuity in Human Cortical Development and Change From Embryonic Stages to Old Age. *Cereb Cortex* **29**, 3879-3890 (2019).
31. S. Elmer, J. Hanggi, M. Meyer, L. Jancke, Increased cortical surface area of the left planum temporale in musicians facilitates the categorization of phonetic and temporal speech sounds. *Cortex* **49**, 2812-2821 (2013).
32. R. Pienaar, B. Fischl, V. Caviness, N. Makris, P. E. Grant, A Methodology for Analyzing Curvature in the Developing Brain from Preterm to Adult. *Int J Imaging Syst Technol* **18**, 42-68 (2008).
33. T. Mediavilla *et al.*, Learning-related contraction of gray matter in rodent sensorimotor cortex is associated with adaptive myelination. *Elife* **11** (2022).
34. V. S. Natu *et al.*, Apparent thinning of human visual cortex during childhood is associated with myelination. *Proceedings of the National Academy of Sciences of the United States of America* **116**, 20750-20759 (2019).
35. K. B. Walhovd, A. M. Fjell, J. Giedd, A. M. Dale, T. T. Brown, Through Thick and Thin: a Need to Reconcile Contradictory Results on Trajectories in Human Cortical Development. *Cereb Cortex* **27**, 1472-1481 (2017).
36. S. A. Valizadeh, F. Liem, S. Merillat, J. Hanggi, L. Jancke, Identification of individual subjects on the basis of their brain anatomical features. *Sci Rep* **8**, 5611 (2018).
37. C. Wachinger *et al.*, BrainPrint: a discriminative characterization of brain morphology. *Neuroimage* **109**, 232-248 (2015).
38. I. Sebenius *et al.*, Structural MRI of brain similarity networks. *Nature reviews. Neuroscience* 10.1038/s41583-024-00882-2 (2024).
39. R. S. Desikan *et al.*, An automated labeling system for subdividing the human cerebral cortex on MRI scans into gyral based regions of interest. *Neuroimage* **31**, 968-980 (2006).

40. A. Raznahan, D. Greenstein, N. R. Lee, L. S. Clasen, J. N. Giedd, Prenatal growth in humans and postnatal brain maturation into late adolescence. *Proceedings of the National Academy of Sciences of the United States of America* **109**, 11366-11371 (2012).
41. P. W. Fox, S. L. Hershberger, T. J. Bouchard, Jr., Genetic and environmental contributions to the acquisition of a motor skill. *Nature* **384**, 356-358 (1996).
42. M. Deppe *et al.*, Increased cortical curvature reflects white matter atrophy in individual patients with early multiple sclerosis. *Neuroimage Clin* **6**, 475-487 (2014).
43. J. B. King, M. P. Lopez-Larson, D. A. Yurgelun-Todd, Mean cortical curvature reflects cytoarchitecture restructuring in mild traumatic brain injury. *Neuroimage Clin* **11**, 81-89 (2016).
44. T. Halevy *et al.*, Twin discordance: a study of volumetric fetal brain MRI and neurodevelopmental outcome. *Eur Radiol* **31**, 6676-6685 (2021).
45. K. F. Casey *et al.*, Birth weight discordance, DNA methylation, and cortical morphology of adolescent monozygotic twins. *Hum Brain Mapp* **38**, 2037-2050 (2017).
46. N. Mukherjee *et al.*, Discordance of prenatal and neonatal brain development in twins. *Early Hum Dev* **85**, 171-175 (2009).
47. W. T. Greenough, J. E. Black, C. S. Wallace, Experience and brain development. *Child development* **58**, 539-559 (1987).
48. Z. Petanjek *et al.*, Extraordinary neoteny of synaptic spines in the human prefrontal cortex. *Proceedings of the National Academy of Sciences of the United States of America* **108**, 13281-13286 (2011).
49. M. S. Yeung *et al.*, Dynamics of oligodendrocyte generation and myelination in the human brain. *Cell* **159**, 766-774 (2014).
50. R. D. Bhardwaj *et al.*, Neocortical neurogenesis in humans is restricted to development. *Proceedings of the National Academy of Sciences of the United States of America* **103**, 12564-12568 (2006).
51. M. F. Paredes, S. F. Sorrells, J. M. Garcia-Verdugo, A. Alvarez-Buylla, Brain size and limits to adult neurogenesis. *J Comp Neurol* **524**, 646-664 (2016).
52. A. E. Rehn *et al.*, An animal model of chronic placental insufficiency: relevance to neurodevelopmental disorders including schizophrenia. *Neuroscience* **129**, 381-391 (2004).
53. K. B. Walhovd *et al.*, Within-session verbal learning slope is predictive of lifespan delayed recall, hippocampal volume, and memory training benefit, and is heritable. *Sci Rep* **10**, 21158 (2020).
54. G. Coughlan *et al.*, Toward personalized cognitive diagnostics of at-genetic-risk Alzheimer's disease. *Proceedings of the National Academy of Sciences of the United States of America* **116**, 9285-9292 (2019).
55. H. J. Spiers, A. Coutrot, M. Hornberger, Explaining World-Wide Variation in Navigation Ability from Millions of People: Citizen Science Project Sea Hero Quest. *Top Cogn Sci* **15**, 120-138 (2023).
56. M. Lovden *et al.*, Spatial navigation training protects the hippocampus against age-related changes during early and late adulthood. *Neurobiol Aging* **33**, 620 e629-620 e622 (2012).
57. S. Scarr-Salapatek, Race, social class, and IQ. *Science* **174**, 1285-1295 (1971).
58. E. M. Tucker-Drob, T. C. Bates, Large Cross-National Differences in Gene x Socioeconomic Status Interaction on Intelligence. *Psychol Sci* **27**, 138-149 (2016).

59. B. G. Rash, J. I. Arellano, A. Duque, P. Rakic, Role of intracortical neuropil growth in the gyrification of the primate cerebral cortex. *Proceedings of the National Academy of Sciences of the United States of America* **120**, e2210967120 (2023).
60. E. Herrera-Luis, K. Benke, H. Volk, C. Ladd-Acosta, G. L. Wojcik, Gene-environment interactions in human health. *Nat Rev Genet* **25**, 768-784 (2024).
61. R. L. Sidman, P. Rakic, Neuronal migration, with special reference to developing human brain: a review. *Brain research* **62**, 1-35 (1973).
62. K. B. Walhovd, M. Lövdén, "A lifespan perspective on human neurocognitive plasticity" in The Cognitive Neurosciences, Gazzaniga, Mangun, Poeppel, Eds. (MIT Press, Cambridge, MA, 2019), https://doi.org/10.7551/mitpress/11442.003.0009 chap. 5.
63. T. Nilsen, I. Brandt, J. R. Harris, The Norwegian Twin Registry. *Twin Res Hum Genet* **22**, 647-650 (2019).
64. M. F. Folstein, S. E. Folstein, P. R. McHugh, "Mini-mental state". A practical method for grading the cognitive state of patients for the clinician. *J Psychiatr Res* **12**, 189-198 (1975).
65. D. Wechsler, *Wechsler abbreviated scale of intelligence* (The Psychological Corporation, San Antonio, TX, 1999).
66. T. S. Nilsen, I. Brandt, P. Magnus, J. R. Harris, The Norwegian Twin Registry. *Twin Res Hum Genet* **15**, 775-780 (2012).
67. T. S. Nilsen, J. Kutschke, I. Brandt, J. R. Harris, Validity of Self-Reported Birth Weight: Results from a Norwegian Twin Sample. *Twin Res Hum Genet* **20**, 406-413 (2017).
68. O. Puonti, J. E. Iglesias, K. Van Leemput, Fast, sequence adaptive parcellation of brain MR using parametric models. *Med Image Comput Comput Assist Interv* **16**, 727-734 (2013).
69. O. Puonti, J. E. Iglesias, K. Van Leemput, Fast and sequence-adaptive whole-brain segmentation using parametric Bayesian modeling. *Neuroimage* **143**, 235-249 (2016).
70. I. Sebenius *et al.*, Robust estimation of cortical similarity networks from brain MRI. *Nat Neurosci* **26**, 1461-1471 (2023).
71. C. R. Madan, Robust estimation of sulcal morphology. *Brain Inform* **6**, 5 (2019).